Journal of Cardiothoracic Surgery

RESEARCH

Open Access

Radiomics integration based on intratumoral and peritumoral computed tomography improves the diagnostic efficiency of invasiveness in patients with pure ground-glass nodules: a machine learning, cross-sectional, bicentric study

Ying Zeng[1†], Jing Chen[2†], Shanyue Lin[3], Haibo Liu[1], Yingjun Zhou[1*] and Xiao Zhou[1*]

Abstract

Background Radiomics has shown promise in the diagnosis and prognosis of lung cancer. Here, we investigated the performance of computed tomography-based radiomic features, extracted from gross tumor volume (GTV), peritumoral volume (PTV), and GTV + PTV (GPTV), for predicting the pathological invasiveness of pure ground-glass nodules present in lung adenocarcinoma.

Methods This was a retrospective, cross-sectional, bicentric study with data collected from January 1, 2018, to June 1, 2022. We divided the dataset into a training cohort ($n = 88$) from one center and an external validation cohort ($n = 59$) from another center. Radiomic signatures (rad-scores) were obtained after features were selected through correlation and least absolute shrinkage and selection operator analysis. Three machine learning models, a support vector machine model, a random forest model, and a generalized linear model, were then applied to build radiomic models.

Results Invasive adenocarcinoma had a higher rad-score ($P<0.001$) in the GTV and GPTV. The area under the curves (AUC) of GTV, PTV, and GPTV were 0.839, 0.809, and 0.855 in the training cohort and 0.755, 0.777, and 0.801 in the external validation cohort, respectively. The GPTV model had higher AUCs for predicting pathological invasiveness. The random forest model had the best validity and fit for the proposed machine learning approach, suggesting that it may be the most appropriate model.

[†]Ying Zeng and Jing Chen contributed equally to this work.

*Correspondence:
Yingjun Zhou
407420879@qq.com
Xiao Zhou
458805788@qq.com

Full list of author information is available at the end of the article

Conclusions GPTV had the highest diagnostic efficiency for predicting pathological invasiveness in patients with pure ground-grass nodules, and the random forest model outperformed other predictive models.

Keywords Computed tomography, Pure ground-glass nodules, Machine learning, Radiomics, Invasiveness

Background

With the development of computed tomography (CT) and widespread use of lung cancer screening programs, early-stage lung adenocarcinomas manifesting as ground-glass nodules (GGNs) are more commonly detected [1, 2]. Among these, pure ground-glass nodules (pGGNs) are defined as focal nodular areas of increased lung attenuation seen on high-resolution CT, revealing the pulmonary vessels and bronchial structures [3, 4]. pGGNs are regarded as indolent lung adenocarcinoma, which is inextricably linked with a pathological predominant lepidic growth [5]. In contrast, 16–27% of pGGNs are pathologically diagnosed with invasive adenocarcinoma (IAC), and lobectomy is recommended in these cases [6–8]. Occasionally, the results of radiologic assessments (such as CT attenuation value, tumor size, and morphological characteristics) may conflict with pathological findings, which are regarded as the "gold standards" of diagnosis and typically guide treatment protocols [3, 4, 9, 10]. Therefore, it is imperative to develop new diagnostic methods with comprehensive and critical information that could improve diagnostic efficiency.

Radiomics refers to the analysis of large volumes of quantitative data extracted from medical images and has shown promising potential in the diagnosis and prognosis of lung cancer [11, 12]. Previous studies have primarily focused on radiomic features within intratumoral regions, often overlooking the peritumoral parenchyma [13, 14]. The investigation of peritumoral radiomic features has garnered increasing attention due to their potential to capture microenvironmental changes in the peritumoral area, which are common attributes of malignancies. Furthermore, the presence of necrotic or hypoxic regions within the central tumor, coupled with predominant cancer cell proliferation in the peripheral tumor, underscores the importance of analyzing peritumoral features [15, 16]. Nagy et al. recently showed that 5-mm peritumoral radiomics can improve the differentiation of adenocarcinoma from granulomas [17]. However, the diagnostic usefulness of peripheral radiomic features for lung adenocarcinoma presenting with GGNs has not been sufficiently explored. Therefore, in this study, we extracted radiomic features from the intratumoral and 5-mm peritumoral regions and applied advanced machine learning approaches. We aimed to assess the performance of radiomic features extracted from these regions in predicting pathological invasiveness in patients with pGGNs. The primary objective of this study was to identify a new diagnostic biomarker capable of accurately predicting the invasiveness of adenocarcinoma on chest CT, thereby providing scientific evidence to support clinical decision-making.

Methods

Study cohort

This bicentric retrospective study was reviewed and approved by the ethics committee of the researchers' hospital. The study adhered to the principles outlined in the Declaration of Helsinki and received approval from the Ethics Committees of the participating hospitals (reference numbers: KY2020147 from The Affiliated Hospital of Southwest Medical University and 2021-07-009 from Xiangtan Central Hospital). Given the retrospective nature of the study and the use of anonymized data, the requirement for informed consent was waived.

The retrospective study involving two centers (The Affiliated Hospital of Southwest Medical University as center 1, Xiangtan Central Hospital as center 2) was conducted from January 1, 2018 to June 1, 2022. All patients whose data was included in the study had undergone a CT scan and surgery. The patients included in this study were required to meet the following criteria: (1) aged 18 years or older; (2) underwent CT scan and subsequent thoracic surgery; (3) had a radiological diagnosis of pure ground glass nodules (pGGNs) on CT imaging; (4) postoperative pathological diagnosis confirmed invasive adenocarcinoma; (5) non-contrast, thin-section chest CT performed within 14 days before surgery; (6) no preoperative chemotherapy, radiotherapy, or chemoradiation; (7) absence of concurrent chronic systemic diseases or other malignancies; and (8) satisfactory quality of the thoracic CT images. Notably, Patients diagnosed with multiple primary lung adenocarcinomas based on postoperative pathology of multiple pGGNs were excluded from the study. A total of 147 patients matched our search criteria. Patients enrolled from center 1 were used as the training cohort ($n = 88$), while those enrolled from center 2 served as the validation cohort ($n = 59$). The study flowchart is presented in Fig. 1.

CT protocol

A series of thin-slice CT scans were performed by different manufacturers using different numbers of detectors, without contrast enhancement, from the apex to the base of the lung. CT scanning was performed using a 64- or 128-slice spiral CT scanner (either Revolution CT [GE Healthcare, Chicago, IL, USA] or MX16 CT [Philips Healthcare, Best, Netherlands] at center 1; uCT550 or

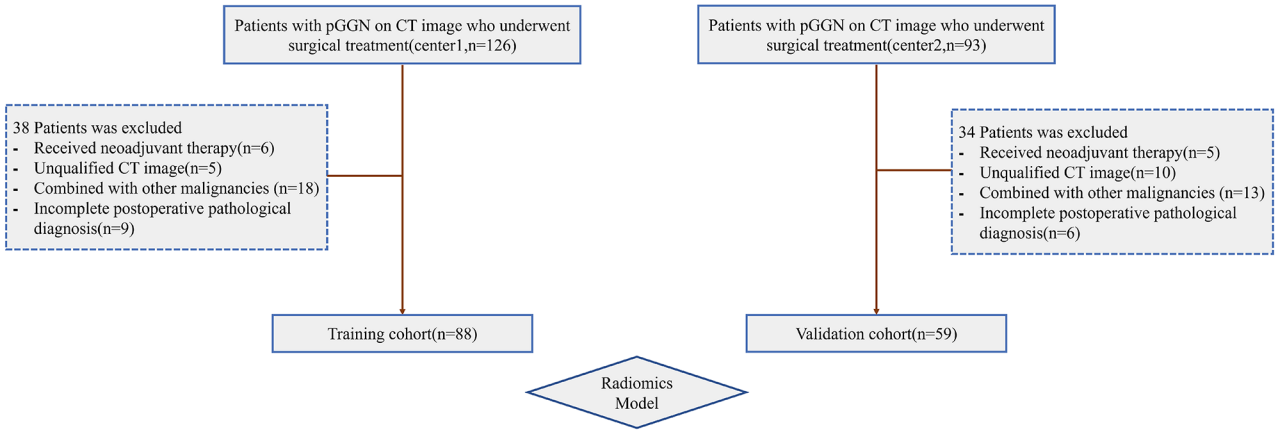

Fig. 1 The diagram below illustrates the study protocol flow for two separate centers. It also includes the inclusion and exclusion criteria for participants at each center

uCT760 [Shanghai United Imaging Healthcare, Shanghai, China] at center 2). For chest CT examination, the following scanning parameters were used: detector collimation, 1–5 mm; beam pitch, 0.75–1.75 mm, 45 keV voltage, 150 mA current, 256 × 512 frames, 500 μs exposure time, and 256 × 512 frame resolution. Reconstructed images had a section thickness of 0.625–1.250 mm and were displayed at 1600 HU, 600 HU, 350 HU, and 35 HU window levels in lung and mediastinal anatomy.

Segmentation and feature extraction

All images in this study were manually segmented using ITK-SNAP software (www.itksnap.org) [18]. The regions of interest (ROIs) were delineated along the nodule boundary on the CT images in horizontal planes by a radiologist specializing in unenhanced chest CT, ensuring that the entire gross tumor volume (GTV) was covered. Following this, another radiologist in the same field reviewed and adjusted the lesion delineation as necessary for quality control. The peritumoral volume (PTV) ROI was defined as the region extending 5 mm outward from the edge of the tumor, while excluding soft tissues such as the chest wall and mediastinum surrounding the tumor [17].

The radiomic features were extracted from GTV and GPTV using the Pyradiomics tool version 3.0, an open-source Python package designed for this purpose. Prior to extract features, all images resampled at a spatial resolution of $1 \times 1 \times 1$ mm^3 and were normalized by calculating their z-scores $[(x - \mu)/\sigma]$, where x denotes the feature value, μ represents the average of feature values among all patients and σ is the corresponding standard deviation. The analysis comprised of first-order and intensity histogram statistics, shape-based features, texture features like gray-level dependence matrix and gray-level size zone matrix, and wavelet-based features [19]. Figure 2 illustrates the flowchart for constructing the radiomic model, encompassing the stages of image selection, image segmentation, feature extraction, feature engineering, as well as model construction and validation.

Dimension reduction was performed using correlation and least absolute shrinkage and selection operator (LASSO) analysis. Pearson correlation analysis was employed for datasets exhibiting normal distribution, whereas Spearman correlation analysis was utilized for datasets with non-normal distribution. Radiomic features demonstrating a correlation coefficient (r) exceeding 0.9 were considered highly correlated, leading to the random exclusion of one of the correlated features [20]. To determine the optimal radiomics signature, the LASSO, a method demonstrated to be effective in the regression analysis of high-dimensional data, was employed. The radiomics features selected through this process were subsequently utilized as inputs for machine learning algorithms in the classification task.

Pathological evaluation

Surgically resected GGN specimens were histopathologically analyzed by an experienced thoracic pathologist according to the revised lung adenocarcinoma (IASLC/ATS/ERS) classification of 2011 [21]. Adenomatous hyperplasia (AAH), adenocarcinomas in situ (AISs), minimally invasive adenocarcinomas (MIAs), and IACs were classified according to the new system. AAH, AIS, and MIA are non-invasive adenocarcinomas (non-IAC), while other types of tumors are IACs.

Statistical analysis

To evaluate the differences in rad-scores between the IAC and non-IAC groups, the study employed both the Student's t-test and the Mann–Whitney U test. Additionally, receiver operating characteristic (ROC) curves were generated, and the corresponding area under the curve (AUC) was calculated to assess the diagnostic

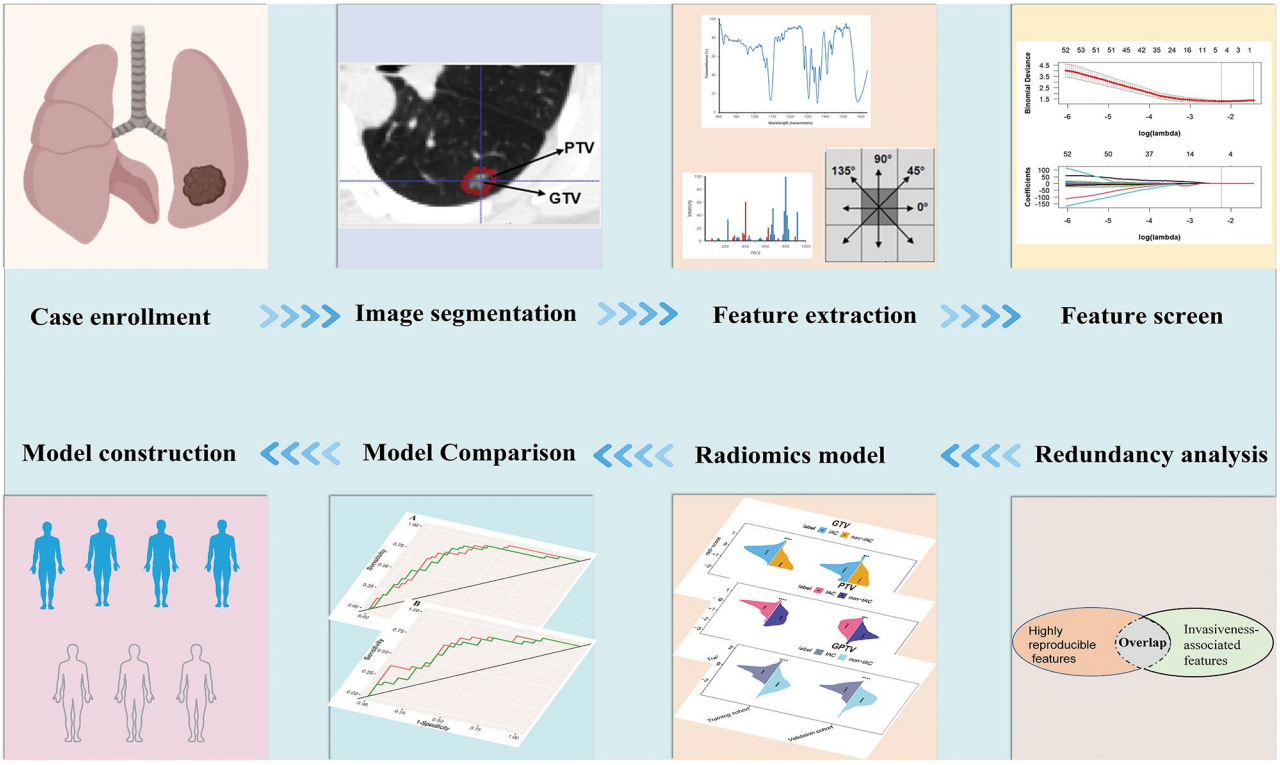

Fig. 2 Workflow of radiomics analysis, including segmentation, feature extraction, feature selection, model building, and model evaluation

Table 1 Baseline data for the training and validation cohort

Variables	Training cohort (*N* = 88)	Validation cohort (*N* = 59)	*p*-value
Sex:			0.499
Male	24 (27.3%)	20 (33.9%)	
Female	64 (72.7%)	39 (66.1%)	
Age:	55.1 (10.4)	54.6 (13.1)	0.805
Location:			0.026
Right upper lobe	34 (38.6%)	17 (28.8%)	
Right lower lobe	9 (10.2%)	15 (25.4%)	
Right middle lung	8 (9.09%)	4 (6.78%)	
Left upper lung	33 (37.5%)	15 (25.4%)	
Left lower lobe	4 (4.55%)	8 (13.6%)	
Pathology:			0.783
Non-IAC	51 (58.0%)	32 (54.2%)	
IAC	37 (42.0%)	27 (45.8%)	
Diameter (mm)	36.9 ± 7.01	36.7 ± 6.69	0.875

Abbreviation: IAC, invasive adenocarcinoma

performance of the rad-score. A p-value of less than 0.05 was considered statistically significant. To understand feature importance, we utilized various machine learning models, including a support vector machine model (SVM), a random forest model (RF), and a generalized linear model (GLM). Furthermore, we employed GridSearch cross-validation (CV), a comprehensive approach that systematically evaluates multiple parameter combinations, with the final selection of hyperparameters based on five-fold CV.

Subsequently, the R package DALEX was applied to explain the three machine learning approaches, and residual distribution was plotted to determine the best model in respect to the validation cohort. In addition, we examined the relative importance of the explanatory features for further study.

Results

Patient characteristics

Our study included 147 patients with pGGNs, 44 (29.93%) men and 103 (70.07%) women (age range, 29–78 years; median age, 56.0 years). Of the 147 cases of lung adenocarcinomas, there were 64 IACs (43.53%), 60 MIAs (40.82%), and 23 AISs (15.65%). The training and validation cohorts did not differ significantly in baseline characteristics (Table 1).

Feature selection and development of the radiomic model.

We extracted 1,222 texture features from the GTV and GPTV. As a result of removal of redundant features based on a correlation coefficient > 0.9, 256 features from GTV, 257 from PTV, and 240 from GPTV were retained.

Afterward, we used LASSO to further reduce the dimensionality of screened features, and a linear combination of the selected features and their coefficients was generated for the rad-score. The rad-scores for the

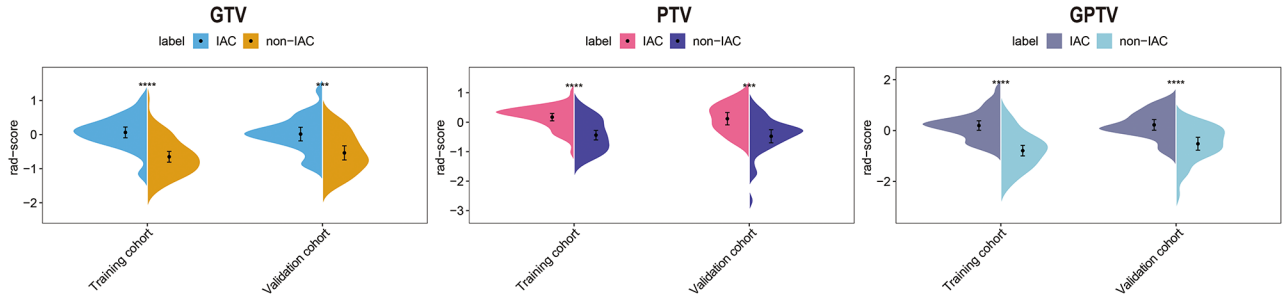

Fig. 3 The violin plot displays the Rad-score of GTV, PTV, and GPTV radiomic models used to differentiate IAC from non-IAC in both the training and validation cohorts. The Rad-score derived from IACs was marginally higher than that obtained from non-IACs

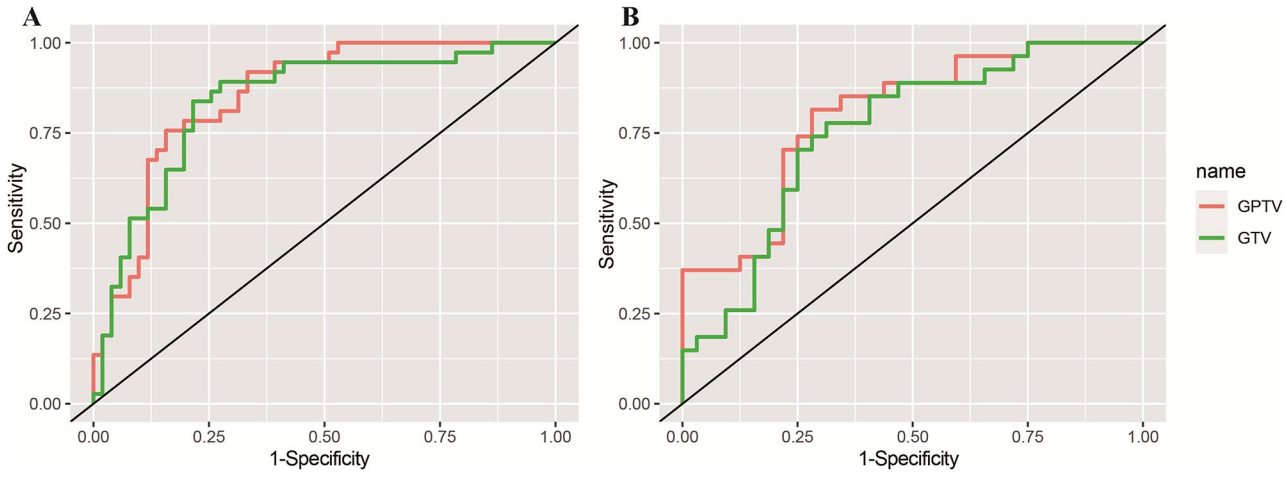

Fig. 4 Receiver operating characteristic (ROC) curve for the GTV, and GPTV radiomic models differentiating IAC from non-IAC, the GPTV radiomics model demonstrated higher performance

Table 2 Diagnostic efficiency of GTV, PTV, and GPTV across training and validation cohort

Radiomic models	Area under curve(95%CI)	Accuracy	Sensitivity	Specificity	Positive predictive value	Negative predictive value
Training cohort						
GTV	0.838(0.821–0.873)	80.68%	83.80%	78.40%	73.80%	87.00%
PTV	0.809(0.792–0.826)	72.72%	85.40%	63.80%	67.30%	83.30%
GPTV	0.855(0.838–0.872)	81.68%	75.70%	84.30%	77.80%	77.80%
Validation cohort						
GTV	0.755(0.729–0.768)	72.88%	77.80%	68.80%	67.70%	78.60%
PTV	0.777(0.701–0.812)	74.58%	78.30%	72.20%	64.30%	83.90%
GPTV	0.801(0.719–0.902)	81.36%	75.70%	84.30%	77.80%	82.70%

Abbreviation: GTV, gross tumor volume; PTV, peritumoral volumes; GPTV, GTV + PTV; CI: confidence intervals

GTV, PTV, and GPTV radiomic models derived from IACs were marginally higher than those derived from non-IACs, in both the training and the validation cohort (P<0.05) (Fig. 3).

Performance and comparison

The GPTV model demonstrated superior performance compared to the GTV model, as evidenced by the AUC values. Specifically, the GPTV model achieved AUCs of 0.855 (95% CI: 0.838–0.872) and 0.801 (95% CI: 0.719–0.902) in the training and validation cohorts, respectively. In contrast, the GTV model yielded AUCs of 0.838 (95% CI: 0.821–0.873) and 0.755 (95% CI: 0.729–0.768) in the corresponding cohorts (Fig. 4A-B). A summary of diagnostic performance is provided in Table 2.

Machine learning approach

The IAC diagnostic model was developed using three machine learning approaches based on GPTV radiomic features: SVM, RF, and GLM. To determine the best model selection in the validation cohort, we visualized the residual distribution. Figure 5(A-B) illustrate that the RF model had the least sample residuals, suggesting that it had the minimal loss function and therefore

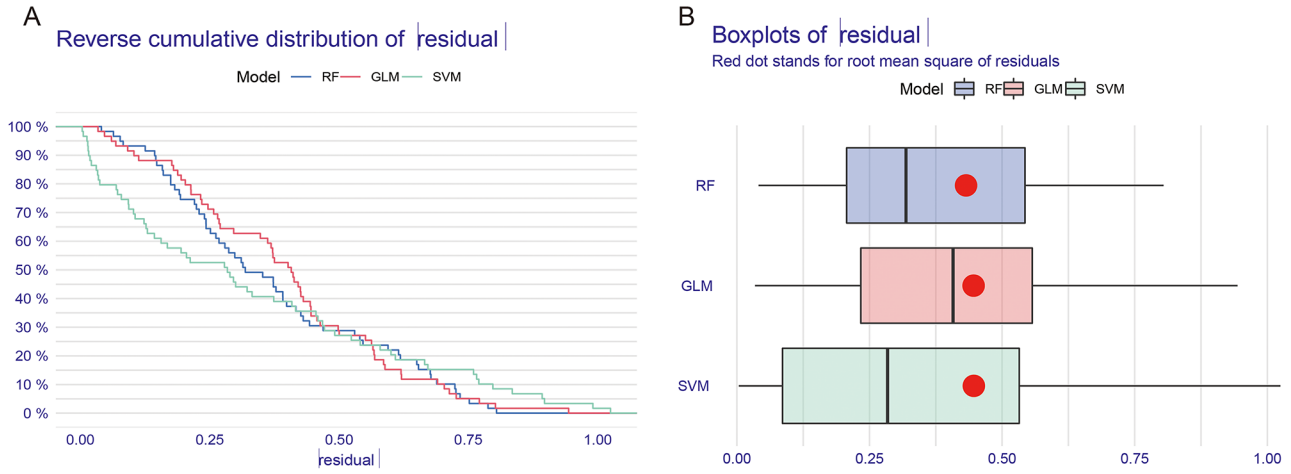

Fig. 5 Construction and assessment of the generalized linear model (GLM), random forest (RF), and support vector machine (SVM) models were conducted. The cumulative residual distribution map the sample was shown in (**A**), while the residuals of the sample were presented in the boxplots in (**B**). The red dot in the boxplots represented the root mean square of residuals

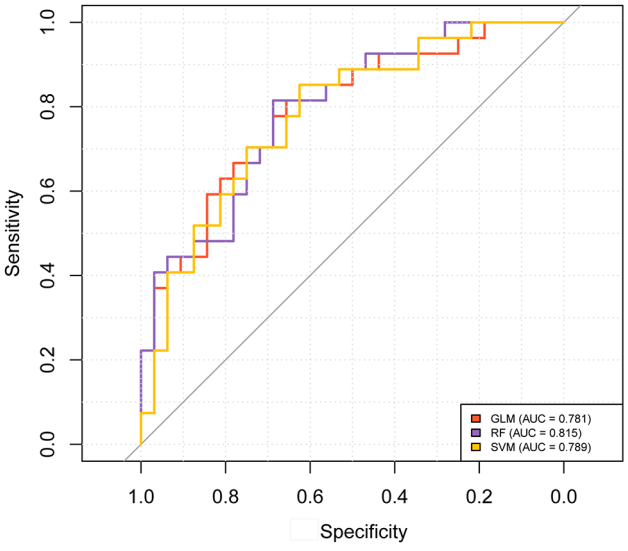

Fig. 6 Receiver operating characteristic (ROC) curve analysis was conducted to evaluate the performance of the radiomics model built using the generalized linear model (GLM), random forest (RF), and support vector machine (SVM) approaches

outperformed the other models tested in predicting IAC. Furthermore, we included ROC curve analysis (Fig. 6) for evaluating diagnostic effectiveness across GLM, RF, and SVM model. The results revealed that RF had the highest area under the curve (0.815), followed by SVM (0.789) and GLM (0.781). These findings validate RF as the top-performing model for diagnostic accuracy. Subsequently, we ranked seven explanatory variables according to their relative importance in the RF model (Fig. 7).

Discussion

In this study, we developed a GTV, PTV, and GPTV radiomic model, cross-validated all three with an external center, and compared the diagnostic efficiency of the different models in differentiating IAC from non-IAC in the training and validation cohorts. Our results show that GPTV had the best diagnostic efficiency in predicting pathological invasiveness in patients with pGGNs. Based on this finding, we developed the IAC diagnostic model using three machine learning approaches.

Persistent pGGNs are usually considered an "indolent" type of lung adenocarcinoma, with annual or biennial CT follow-up recommended as a management approach [5]. Approximately 16–27% of pGGNs are pathologically diagnosed with IAC, and some radiographical signs, such as pleural invasion, spiculation lobulation, the notch sign, and bubble-like sign, are associated with pathological invasiveness [22–24]. The interpretation of these characteristics, however, is prone to inter- and intra-observer variability based on the experience and expertise level of the radiologist [24].

Radiomic features have the potential to provide phenotypic information through high-throughput algorithms, describing additional tumor characteristics that may go unnoticed by radiologists. This potential impact on the clinical management of lung adenocarcinoma lies in the utilization of intranodular and perinodular radiomic features. These features can enhance diagnostic accuracy, prognostic stratification, treatment selection, and therapy monitoring [24]. Intratumoral radiomic features have shown promising potential in differentiating IACs from non-IACs, which is consistent with the result of the current study [13, 14]. In recent years, peritumoral radiomic features have gradually gained attention as a burgeoning biomarker of the radiomics method. Nagy et al. showed

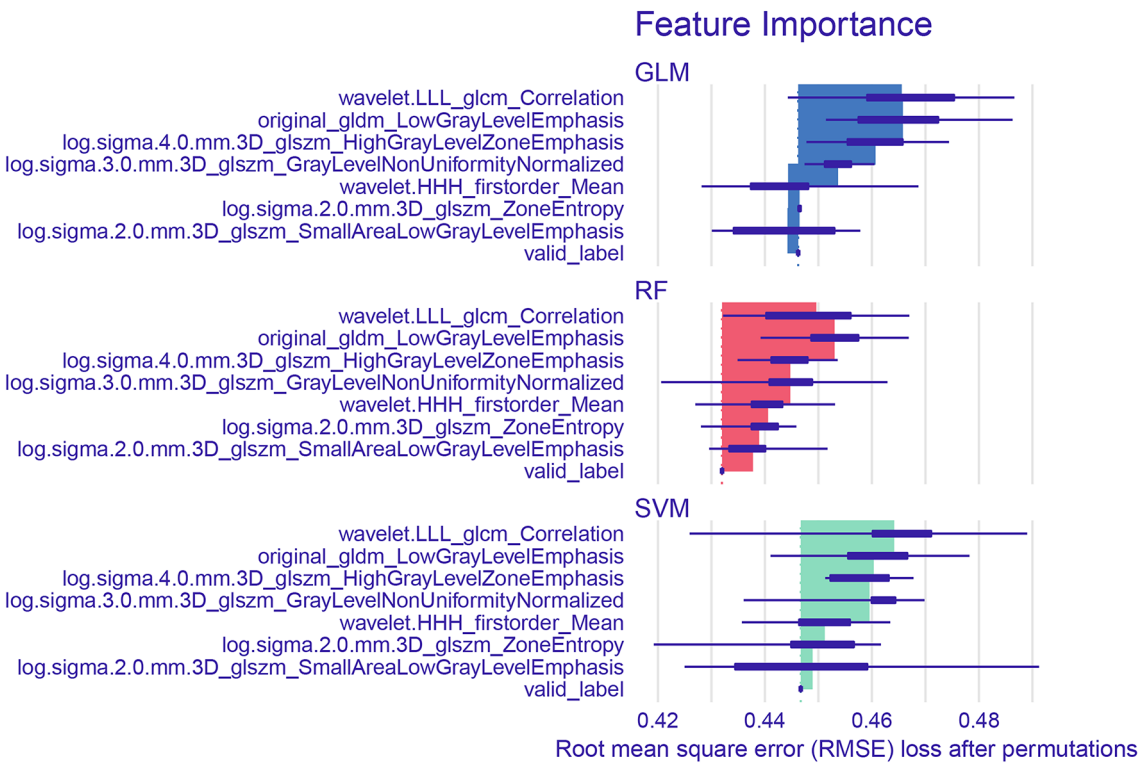

Fig. 7 The relative importance of explanatory variables in the generalized linear model (GLM), random forest (RF), and support vector machine (SVM) models were assessed, with each model providing an importance ranking for the identified radiomics features

that 5-mm peritumoral radiomics can increase efficiency in differentiating adenocarcinoma from granulomas (intranodular radiomic vs. perinodular radiomic: 0.75 vs. 0.80) [17]. Das et al. [25] found that the integration of GPTV further improved the discriminatory ability for predicting lymph node involvement in cT1N0M0 lung adenocarcinomas (GPTV vs. GTV vs. PTV: 0.75 vs. 0.74 vs. 0.72). Wu et al. [26] indicated that the peritumoral parenchymal region within 5 mm of the tumor contained useful information that could predict the pathological invasiveness of lung adenocarcinoma manifesting as pGGNs. Based on the results of the above-mentioned studies, the integration of GTV and 5-mm PTV was applied in the present study. We discovered that patients diagnosed with IAC generally had a significantly higher rad-score than those not diagnosed with IAC; the same result was confirmed in the validation cohort. Furthermore, among the various radiomic models, GPTV demonstrated the highest diagnostic efficiency. This finding suggests that incorporating radiomic features extracted from both the intratumoral and peritumoral regions can supplement tumor-based features by capturing additional information about the microenvironment of surrounding tissues, such as tissue density, heterogeneity, and vascularity. These captured features may reflect crucial biological processes like tumor infiltration, angiogenesis, and inflammation, which have implications for clinical outcomes and treatment response. Therefore, integrating peritumoral features into a radiomic model has the potential to enhance diagnostic efficiency.

Owing to GPTV having the highest diagnostic efficiency, the IAC diagnostic model was developed using three machine learning approaches based on GPTV radiomic features. When integrated into machine learning, GPTV radiomic features can reduce data requirements, increase reliability, and improve the reliability and robustness of machine learning systems. In this study, the RF model outperformed the other models in terms of machine learning and the relative importance of explanatory variables.

However, this study has some limitations. First, due to the bicentric retrospective design employed. Variations in CT scanning protocols, differences in image quality, and demographic disparities between the two centers could lead to variability in the results and limit their generalizability to other clinical populations and healthcare settings. Second, ROI demarcation was performed visually and by manual delineation in several steps, which could have led to interobserver variability, limiting its clinical usefulness. Third, owing to the retrospective nature of the study, there were limitations to the data we were able to collect. Therefore, multicenter studies are needed to improve the database needed to train the artificial intelligence system in the future to

prevent selection bias. Finally, the utilization of GPTV models in clinical practice holds potential benefits such as improved patient outcomes, reduced healthcare costs, and increased efficiency. However, it is important to conduct further studies to confirm the clinical utility of the model and assess its impact on patient outcomes. This will provide a more comprehensive understanding of its potential implications.

Conclusion

In conclusion, the integration of GTV and PTV increases the performance of both in predicting the pathological invasiveness of lung adenocarcinoma manifesting as pGGNs. This study underscores the importance of considering radiomic features from both intratumoral and peritumoral regions in distinguishing pathological invasiveness. Furthermore, our findings indicate that the RF machine learning approach is a reliable, practical, and cost-effective tool for the individualized management of pGGNs.

Abbreviations

GGNs	Ground glass nodules
PGGNs	Pure ground-glass nodules
IAC	Invasive adenocarcinoma
GTV	Gross tumor volume
ROIs	Regions of interest
PTV	Peritumoral volume
LASSO	Least absolute shrinkage and selection operator
AAH	Adenomatous hyperplasia
AISs	Adenocarcinomas in situ
MIAs	Minimally invasive adenocarcinomas
RF	Random forest model
SVM	Support vector machine model
GLM	Generalized linear model

Author contributions

Ying Zeng, Jing Chen, Yingjun Zhou and Xiao Zhou wrote the main manuscript text and prepared figures and tables. All authors reviewed the manuscript.

Funding

This work was partly supported by Sichuan Science and Technology Program(2022YFS0616).

Data availability

We confirm that the data and materials used in this study are available upon reasonable request to the corresponding author, pending permission from our institutional review board and the parties involved with the data sharing. The raw data cannot be made publicly available due to ethical and legal restrictions, as they contain identifiable patient information. However, we have provided a comprehensive description of our experimental design, analysis procedures, and results in the manuscript, and supplementary material, to promote transparency and facilitate reproducibility to the best of our abilities.

Declarations

Ethical approval

The study design was approved by the appropriate ethics review board. We have read and understood your journal's policies, and we believe that neither the manuscript nor the study violates any of these.

Competing interests

The authors declare no competing interests.

Author details

[1]Department of Radiology, Xiangtan Central Hospital, Xiangtan, Hunan 411000, China
[2]Department of Radiology, The Affiliated Hospital of Southwest Medical University, Luzhou, Sichuan 646000, China
[3]Department of Radiology, Affiliated Hospital of Guilin Medical University, Guilin, Guangxi 541001, China

Received: 20 June 2023 / Accepted: 25 December 2024
Published online: 11 February 2025

References

1. Callister ME, Baldwin DR, Akram AR, et al. British Thoracic Society guidelines for the investigation and management of pulmonary nodules. Thorax. 2015;70(Suppl 2):ii1–54. https://doi.org/10.1136/thoraxjnl-2015-207168.
2. Gould MK, Tang T, Liu IL, et al. Recent trends in the identification of Incidental Pulmonary nodules. Am J Respir Crit Care Med. 2015;192:1208–14. https://doi.org/10.1164/rccm.201505-0990OC.
3. Han L, Zhang P, Wang Y, et al. CT quantitative parameters to predict the invasiveness of lung pure ground-glass nodules (pGGNs). Clin Radiol. 2018;73:504. https://doi.org/10.1016/j.crad.2017.12.021.
4. Fu F, Zhang Y, Wang S, et al. Computed tomography density is not associated with pathological tumor invasion for pure ground-glass nodules. J Thorac Cardiovasc Surg. 2021;162:451–e4593. https://doi.org/10.1016/j.jtcvs.2020.04.169.
5. Kitazawa S, Saeki Y, Kobayashi N, et al. Three-dimensional mean CT attenuation value of pure and part-solid ground-glass lung nodules may predict invasiveness in early adenocarcinoma. Clin Radiol. 2019;74:944–9. https://doi.org/10.1016/j.crad.2019.09.130.
6. Kitami A, Sano F, Hayashi S, et al. Correlation between histological invasiveness and the computed tomography value in pure ground-glass nodules. Surg Today. 2016;46:593–8. https://doi.org/10.1007/s00595-015-1208-1.
7. Lee GD, Park CH, Park HS, et al. Lung adenocarcinoma invasiveness risk in pure ground-glass opacity lung nodules smaller than 2 cm. Thorac Cardiovasc Surg. 2019;67:321–8. https://doi.org/10.1055/s-0037-1612615.
8. Heidinger BH, Anderson KR, Nemec U, et al. Lung adenocarcinoma manifesting as pure ground-glass nodules: correlating CT size, volume, density, and roundness with histopathologic Invasion and size. J Thorac Oncol. 2017;12:1288–98. https://doi.org/10.1016/j.jtho.2017.05.017.
9. Zhou QJ, Zheng ZC, Zhu YQ, et al. Tumor invasiveness defined by IASLC/ATS/ERS classification of ground-glass nodules can be predicted by quantitative CT parameters. J Thorac Dis. 2017;9:1190–200. https://doi.org/10.21037/jtd.2017.03.170.
10. Liu Y, Sun H, Zhou F, et al. Imaging features of TSCT predict the classification of pulmonary preinvasive lesion, minimally and invasive adenocarcinoma presented as ground glass nodules. Lung Cancer. 2017;108:192–7. https://doi.org/10.1016/j.lungcan.2017.03.011.
11. Hassani C, Varghese BA, Nieva J, Duddalwar V. Radiomics in Pulmonary Lesion Imaging. AJR Am J Roentgenol. 2019;212:497–504. https://doi.org/10.2214/AJR.18.20623.
12. Thawani R, McLane M, Beig N, et al. Radiomics and radiogenomics in lung cancer: a review for the clinician. Lung Cancer. 2018;115:34–41. https://doi.org/10.1016/j.lungcan.2017.10.015.
13. Fan L, Fang M, Li Z, et al. Radiomics signature: a biomarker for the preoperative discrimination of lung invasive adenocarcinoma manifesting as a ground-glass nodule. Eur Radiol. 2019;29:889–97. https://doi.org/10.1007/s00330-018-5530-z.
14. Gong J, Liu J, Hao W, et al. Computer-aided diagnosis of ground-glass opacity pulmonary nodules using radiomic features analysis. Phys Med Biol. 2019;64:135015. https://doi.org/10.1088/1361-6560/ab2757.
15. Mittal V, El Rayes T, Narula N, et al. The Microenvironment of Lung Cancer and therapeutic implications. Adv Exp Med Biol. 2016;890:75–110. https://doi.org/10.1007/978-3-319-24932-2_5.
16. Altorki NK, Markowitz GJ, Gao D, et al. The lung microenvironment: an important regulator of tumour growth and metastasis. Nat Rev Cancer. 2019;19:9–31. https://doi.org/10.1038/s41568-018-0081-9.
17. Beig N, Khorrami M, Alilou M, et al. Perinodular and Intranodular Radiomic Features on lung CT images distinguish adenocarcinomas from Granulomas. Radiology. 2019;290:783–92. https://doi.org/10.1148/radiol.2018180910.

18. Yushkevich PA, Piven J, Hazlett HC, et al. User-guided 3D active contour segmentation of anatomical structures: significantly improved efficiency and reliability. NeuroImage. 2006;31:1116–28. https://doi.org/10.1016/j.neuroimage.2006.01.015.
19. van Griethuysen JJM, Fedorov A, Parmar C, et al. Computational Radiomics System to Decode the Radiographic phenotype. Cancer Res. 2017;77:e104–7. https://doi.org/10.1158/0008-5472.
20. Cen C, Liu L, Li X, et al. Pancreatic ductal adenocarcinoma at CT: a combined Nomogram Model to Preoperatively Predict Cancer Stage and Survival Outcome. Front Oncol. 2021;11:594510. https://doi.org/10.3389/fonc.2021.594510.
21. Travis WD, Brambilla E, Noguchi M, et al. International association for the study of lung cancer/american thoracic society/european respiratory society international multidisciplinary classification of lung adenocarcinoma. J Thorac Oncol. 2011;6:244–85. https://doi.org/10.1097/JTO.0b013e318206a221.
22. Nelson DB, Godoy MCB, Benveniste MF, et al. Clinicoradiographic predictors of Aggressive Biology in Lung Cancer with Ground Glass Components. Ann Thorac Surg. 2018;106:235–41. https://doi.org/10.1016/j.athoracsur.2018.02.020.
23. Antonoff MB. The search for reliable markers of ground glass opacity prognosis: the truth remains largely unknown. J Thorac Cardiovasc Surg. 2018;156:814–5. https://doi.org/10.1016/j.jtcvs.2018.03.020.
24. van Riel SJ, Ciompi F, Winkler Wille MM, et al. Malignancy risk estimation of pulmonary nodules in screening CTs: comparison between a computer model and human observers. PLoS ONE. 2017;12:e0185032. https://doi.org/10.1371/journal.pone.0185032.
25. Das SK, Fang KW, Xu L, Li B, Zhang X, Yang HF. Integrative nomogram of intratumoral, peritumoral, and lymph node radiomic features for prediction of lymph node metastasis in cT1N0M0 lung adenocarcinomas. Sci Rep. 2021;11:10829. https://doi.org/10.1038/s41598-021-90367-4.
26. Wu L, Gao C, Ye J, et al. The value of various peritumoral radiomic features in differentiating the invasiveness of adenocarcinoma manifesting as ground-glass nodules. Eur Radiol. 2021;31:9030–7. https://doi.org/10.1007/s00330-021-07948-0.

Publisher's note